Improved Sensorless Control of a Modular Three Phase Radial Active Magnetic Bearing

Matthias Hofer, Markus Hutterer, Thomas Nenning, Manfred Schrödl

Institute of Energy Systems and Electric Drives, Vienna University of Technology,
Gusshausstraße 25, 1040 Vienna, Austria,
matthias.hofer@tuwien.ac.at

***Abstract*—This paper discusses new results and improvements on the sensorless control of a permanent magnet biased three phase radial active magnetic bearing (AMB), which are also known as hybrid magnetic bearings (HMB). Self-sensing methods offer cost potentials because of a more simple bearing system architecture, but show lower performance in accuracy and bandwidth compared to external position sensors. Thus, making self-sensing technologies competitive to systems with position sensors is a broad field of research and as well a goal of this paper. The proposed sensorless method is based on inductance measurement by voltage pulse injection. Applying an oversampling strategy for current slope measurement reduces the noise of the sensorless obtained rotor position significantly. Timing limitations and operational bandwidth can be improved by utilizing alternative voltage pulse sequences. Further, variations of the permanent magnet bias flux of the HMB prototype are investigated to show the influences on the sensorless rotor position detection method and limitations for applications.**

I. Introduction

Active magnetic bearings are used for levitation of rotating shafts. Usually they are used in applications where classical technologies are not useful, especially at high operational speeds and/or under high environmental requirements [1]. Here the advantages of a frictionless and a wearless mechanical support with low maintenance and additional functionality like active balancing are utilized. Definitely, compared to classical bearing types the AMB system is more complex and has higher costs. One potential for cost reduction is found in the self-sensing technology which reduces the number of components and increase utilization of of already used components. In general, sensorless means, that the electromagnetic actuator itself is used as position sensor too and rotor position information is evaluated by electrical quantities, namely currents and voltages. Thus, external position sensors are avoided. At AMB applications the position sensing system takes over a major functionality. First because of the unstable positioning behavior at ferromagnetic levitation systems. And second, the sensor parameters affect the overall AMB system and its operation boundaries like bandwidth, noise, accuracy, etc. Thus, self-sensing or respectively sensorless technologies for AMBs are field of research since many years [2] with the target to reach parameters as sensor systems do have. The sensorless control approach used in this work is based on the so called INFORM (Indirect Flux detection by Online Reactance Measuremnt) method which is known from sensorless control of electrical drive applications. At AMBs this method allows the rotor position determination during voltage injection pulses by using a three phase bearing architecture (Fig. 1) together with a three phase voltage source inverter similar to electric drives [3], [4]. Hence, using common inverter technology offers a further cost reduction potential. A short introduction in the INFORM method at AMB is given at the beginning of this work. First, alternative voltage injection sequences and their position sensing accuracy are discussed. Limitation factors for self-sensing performance are already known from literature [5], [6]. Especially nonlinearities like saturation have high impact on self-sensing technologies. Therefore one goal of this work is to identify the impact of high flux levels or even saturation on the sensorless obtained rotor position by the INFORM method.

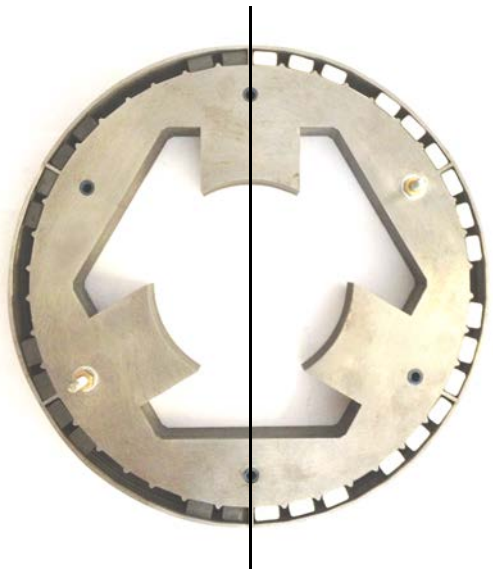

Figure 1. Stator lamination with various permanent magnet configurations - left: N_M=24 ferrite magnets, right: N_M=36 NdFeB magnets

II. Active Magnetic Bearing Design

In this work a three phase permanent magnet biased homopolar AMB with a modular approach is used. By utilizing exchangeable permanent magnets according to Fig. 1 instead of a permanent magnet ring , e.g. as shown in [7], the bias flux level can be adjusted. A wide bias flux range is

reached by varying the number of magnets N_M and even the magnet types according to Tab. I. Combined with different coil configurations a variable and modular bearing setup is given which enables the identification of parameter dependencies and possible operating limits of the sensorless control method.

Table I
BEARING SETUP FOR DIFFERENT BIAS FLUX - ANALYTICAL MODEL

N_M	Magnet type	Bias flux density B_0
12	Ferrite	0.079 T
24	Ferrite	0.182 T
36	Ferrite	0.269 T
12	NdFeB	0.319 T
24	NdFeB	0.649 T
36	NdFeB	0.949 T

The bias flux density B_0 affects the bearing force characteristic of the AMB, e.g the force behavior in x direction (vertical) is shown in Fig. 2. As known, at increasing bias flux density B_0 the force generation per phase current increases. Consequently the force current stiffness factor K_i gets higher for permanent magnet biased bearings and result in a lower current consumption and higher bearing efficiency.

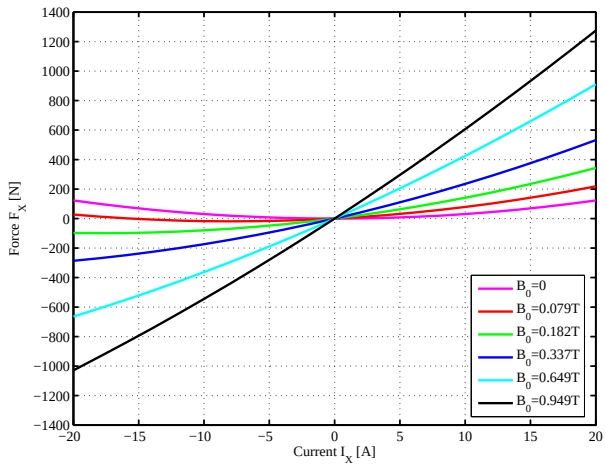

Figure 2. Modeled bearing forces F_X at various permanent magnet configurations for a coil with N=20 turns

In Fig. 3 the phase current for several bias flux densities B_0 is modeled. Additionally measurement results for the AMB prototype setup with N_M=24 Ferrite magnets show a bias current of I_{X0}=7.5A. For another setup with higher premagnetization by using a combination of 12 ferrite and 12 NdFeB magnets per stator stack the bias current consumption is reduced to I_{X0}=4.65A. These measurements confirm the principle behavior of the analytical model, although the measured current consumption is slightly higher due to model uncertainties.

III. SENSORLESS CONTROL METHOD

A. Sensorless position detection

For the capability of a sensorless rotor position detection the AMB stator inductance dependency on the rotor position has

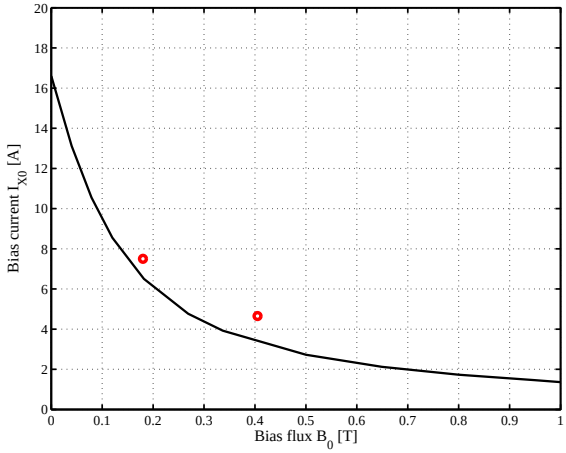

Figure 3. Bias Current I_{X0} for several bias flux densities B_0 at N=20 turns for a rotor weight $m = 8.64$kg- analytical model (black) and measurement results (red).

to be considered. Using a two axis notation the flux linkages ψ_X and ψ_Y derive as

$$\begin{aligned} \psi_X &= L_{XX} \cdot I_X + L_{XY} \cdot I_Y \\ \psi_Y &= L_{YX} \cdot I_X + L_{YY} \cdot I_Y \end{aligned} \tag{1}$$

with the self inductances L_{XX}, L_{YY} and the cross coupling inductances $L_{XY} = L_{YX}$. Herein, the complex stator current space phasor is represented by the components I_X and I_Y. For measuring the inductance characteristic and its position dependency the inverse inductance is helpful. Using the nominal inductance L_0 at centered rotor the inverse of the rated self inductance is build as

$$\frac{1}{l_{XX}|_{y=0}} = \frac{L_0}{L_{XX}} \tag{2}$$

An analysis of the analytic electromagnetic AMB model show a dependency on the rotor position x according to Fig. 4. For an ideal permeable iron ($\mu_{r,Fe} \to \infty$) a simple characteristic is given at a nominal airgap δ_0 as

$$\frac{1}{l_{XX}|_{y=0}} = 1 - \frac{x}{2\delta_0} \tag{3}$$

Changing the relative permeability of the iron path from an ideal permeable material to a real parameter value of e.g. $\mu_{r,Fe} = 1000$ a reduction of the position sensitivity is identified. Thus, to reach high accuracy in self-sensing the relative permeability should be as high as possible. To evaluate the rotor displacement out of this fundamental characteristic a linear combination of three current slope measurements in each phase direction U, V and W is used.

B. Symmetric voltage pulses

A typical current response during an applied symmetric voltage injection pulse sequence is shown in Fig. 5. For a measurement in x direction (aligned with phase direction U) a voltage space phasor pattern $\underline{u}_{u-} \to \underline{u}_{u+} \to \underline{u}_{u-} \to \underline{u}_{u+}$ is applied. This classical pulse sequence result in a symmetric current slope detection around the operation point.

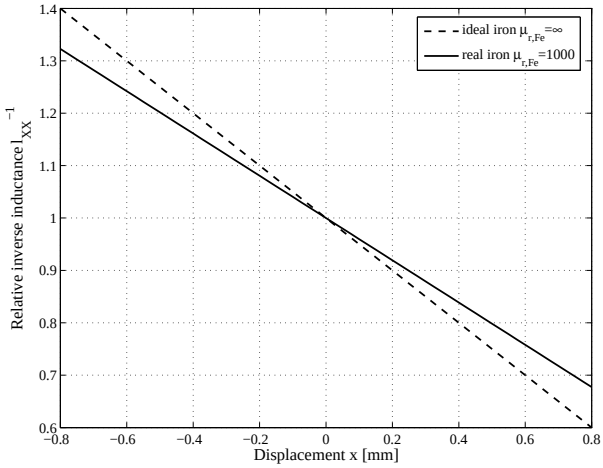

Figure 4. Relative inverse inductance ${l_{XX}}^{-1}$ analytically derived. Dependency on the rotor position $x|_{y=0}$ for ideal permeable material and $\mu_{r,Fe} = 1000$

The measured current response show eddy current effects immediately after each voltage switching. Therefore current slope measurement is only performed in the "linear" range of the current response, but this reduces the sensitivity compared to the maximum theoretical value without eddy currents.

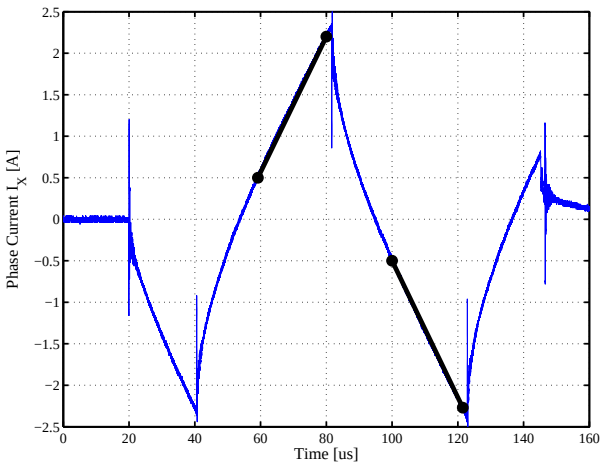

Figure 5. Inductance measurement of $L_{XX}|_{y=0}$ by symmetric voltage pulse injections at position $x = 0.8mm$, U_{DC}=120 V. Measured current reaction I_X and linear current slope approximation by two single samples per slope (black)

C. Asymmetric voltage pulses

Alternative to a symmetric pulse pattern a shortened asymmetric pulse sequence can be used as depicted in Fig. 6. Here the current slope is not measured symmetrically around the magnetic operation point due to eddy current effects. By shortening the pulse sequence duration the position measurement frequency can be increased for improving self-sensing bandwidth but the signal content for slope detection is only half compared to the symmetric voltage pulses.

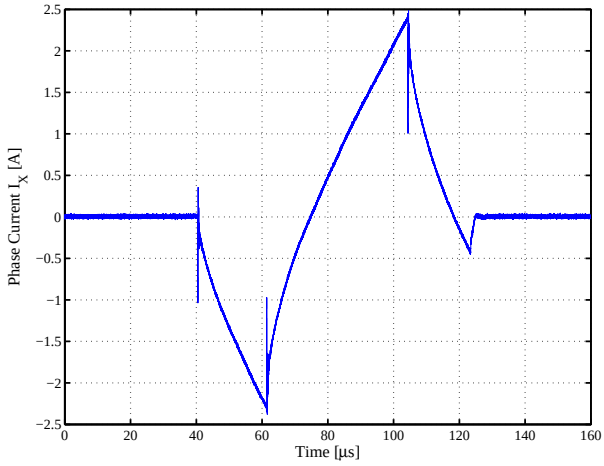

Figure 6. Inductance measurement of $L_{XX}|_{y=0}$ by asymmetric voltage pulse injections at position $x = -0.4mm$ at U_{DC}=120 V. Measured current reaction I_X.

D. Three active voltage pulses

The three active sequence applies voltage space phasors in all three phase directions within one sequence. E.g using negative space phasors $\underline{u}_{u-} \rightarrow \underline{u}_{v-} \rightarrow \underline{u}_{w-}$ the current slopes Δi_U, Δi_V and Δi_W are available immediately and result in a higher self sensing bandwith at the same pulse rate. Using pre-phasors and post-phasors according to Fig. 7 the slope measurements are symmetric around the operation point. The measured current reaction is depicted in Fig. 8.

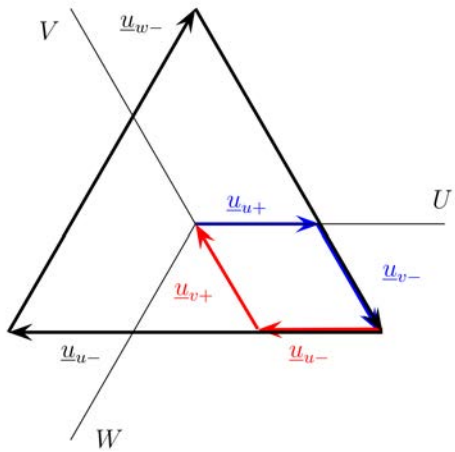

Figure 7. Voltage space phasors for three active voltage pulse injection including pre-phasors (blue) and post-phasors (red) achieving symmetric operation points

E. Noise reduction by oversampling

New digital signal processors (DSPs) offer fast analog to digital conversions (ADC) with high resolution. Therefore increasing the number of samples during the voltage pulse sequence is feasible. This oversampling strategy reduces the noise of the sensorless determined rotor position for same pulse pattern as shown in Tab. II. Here statistical methods

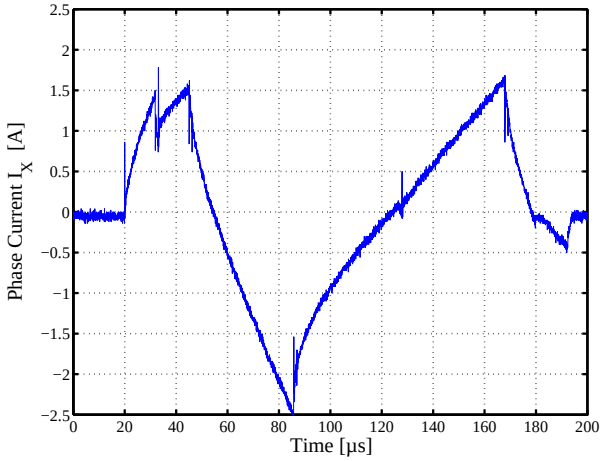

Figure 8. Inductance measurement $L_{XX}|_{y=0}$ by three active voltage pulse injections at position $x = -0.4mm$ at U_{DC}=120 V. Measured current reaction I_X.

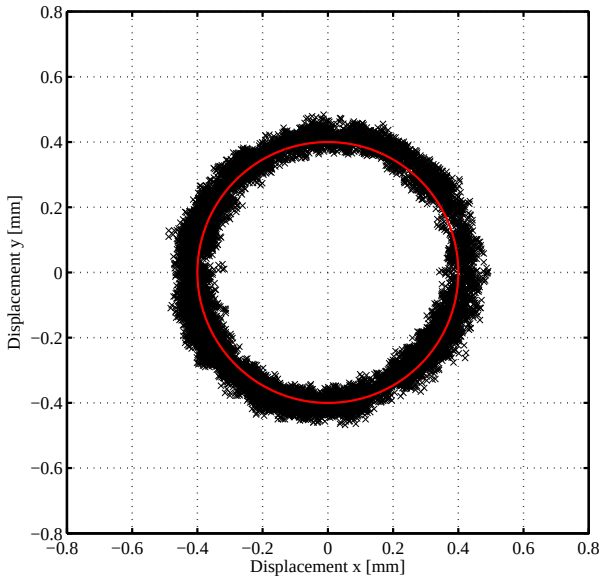

Figure 9. Trajectory of the sensorless position measurements with double sampling and symmetric voltage pulses at radial rotor displacements r=0.4mm for a setup with N_M=24 ferrite magnets (black). Rotor displacement (red).

are used to evaluate the accuracy of the sensorless rotor position according [8]. A standard deviation of σ=25 μm can be reduced to σ=15 μm by changing from a double sampling strategy to quad sampling for symmetric pulses. Depending on electronic hardware capabilities (computation power of the DSP and the ADC) current sampling even up to a continuous oversampling of the current signal during the injected voltage pulse can offer further improvements.

Table II
STANDARD DEVIATION OF THE ROTOR POSITION FOR DIFFERENT INFORM PULSES

Pulse type	Sampling	Std. dev. σ	Bearing setup
symmetric	2	25 μm	24 ferrites
symmetric	4	15 μm	24 ferrites
symmetric	4	12 μm	12 ferrites, 12 NdFeB
symmetric	8	11 μm	12 ferrites, 12 NdFeB
asymmetric	4	19 μm	24 ferrites
asymmetric	4	19 μm	12 ferrites, 12 NdFeB
asymmetric	8	19 μm	12 ferrites, 12 NdFeB
three active	16	8 μm	12 ferrites, 12 NdFeB

The sensorless position signal accuracy can also be evaluated considering mechanically defined rotor positions. Measurement results in Tab. II show the position noise at one mechanical fixed rotor position. Alternatively trajectories at certain radial displacements are used to discuss the self sensing positon accuracy. Such trajectories for a radial displacement of r=0.4 mm (40 % of the airgap defined by touchdown bearings) are depicted in Fig. 9, Fig. 10 and Fig. 11 for different voltage pulse sequences and number of current slope samples.

For the sensorless control of the permanent magnet biased AMB prototype a three phase voltage source inverter with digital control is used. The current measurement is implemented with shunt resistors at the low side switches according to Fig. 12. This current sensing architecture is advantageous for current slope measurement during negative voltage phasors $\underline{u}_{u-}, \underline{u}_{v-}$ and $\underline{u}_{w-}$ because here the phase currents can be measured directly. At positive voltage space phasors the phase currents have to be evaluated indirectly out of the other two phase currents. For this reason the position measurement by the three active sequence allows higher number of current samples of the sequential ADC and result in a higher position accuracy.

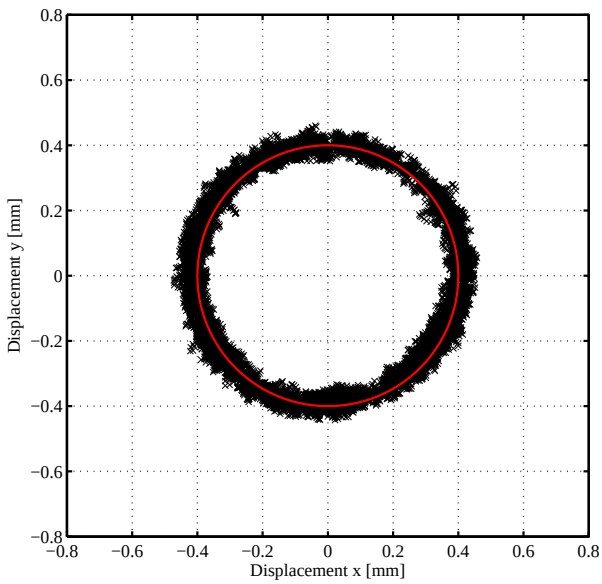

Figure 10. Trajectory of the sensorless position measurements with quad sampling and asymmetric voltage pulses at radial rotor displacements r=0.4mm for a setup with N_M=24 ferrite magnets (black). Rotor displacement (red).

IV. BIAS FLUX INFLUENCE ON THE SENSORLESS ROTOR POSITION

Permanent magnet biased AMBs can achieve high load forces and and a high current force coefficient K_i at relatively

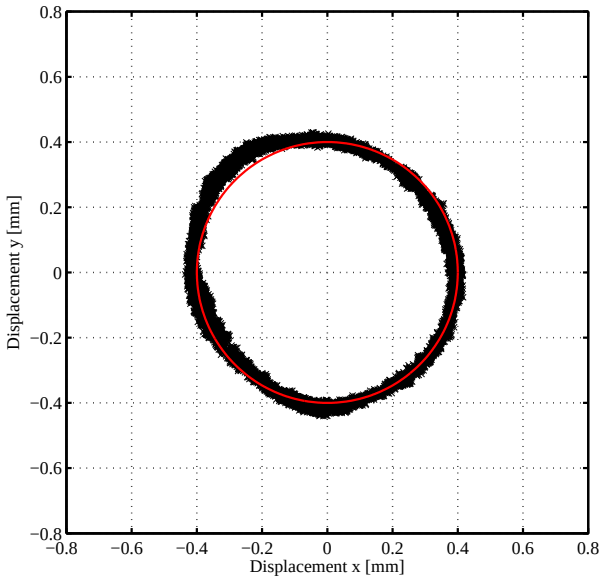

Figure 11. Trajectoriy of the sensorless position measurements with 16 samples at three active voltage pulses at radial rotor displacements r=0.4mm for a setup with 12 ferrite magnets (black). Rotor displacement (red).

small bearing dimensions. Thus a high utilization of the magnetic materials with high flux density levels is given and can lead to saturation. As saturation of the iron path influences self sensing performance [5], [6] this behavior and possible limitations for the applied sensorless method are a main interest in this work too. According to Tab. II a comparison of two different bias flux levels is given for several voltage pulse sequences. The increased bias flux level do not affect the self sensing position noise in the open loop, but the trajectory shape is slightly deformed at the higher bias flux as shown in Fig. 11.

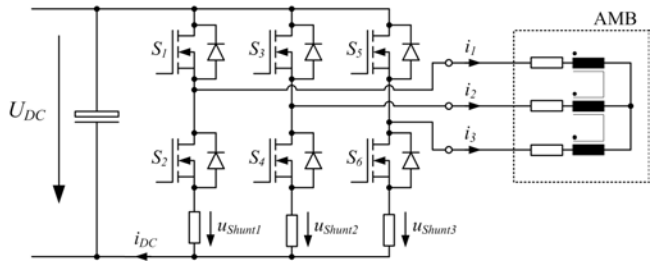

Figure 12. Three phase inverter with current measurement at the low side switches.

V. Sensorless Position Control

The investigation of improvents on the closed loop behvaior is performed with the AMB prototpye as depicted in Fig. 13. First the sensorless PID position control is discussed at the bearing setup with low bias flux and the classical symmetric INFORM pulse sequence. In Fig. 14 a step response from $\pm 0.2mm$ (20% of the airgap) is depicted. The position signal does only contain position sensing noise which is not much higher than in the open loop and no clear oscillations are identified. Despite the low bias flux and low gain of the position controller the load capacity is low.

The sensorless control with asymmetric INFORM pulses at

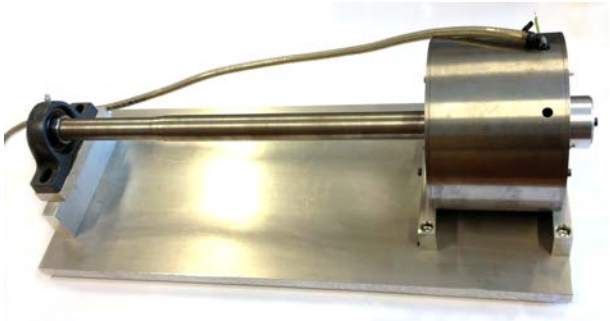

Figure 13. Laboratory setup of the homopolar three phase AMB.

centered rotor is presented in Fig. 15. The position detection rate is increased compared to the symmetric pulses, but according to Tab. II the position noise is much higher even with 8 current samples. This measurement is done at higher bias flux, where the position noise result in high oscillations at levitation. Definitely the maximum bearing load is increased, but the control behavior looks nervous.

The sensorless control behavior with three active INFORM

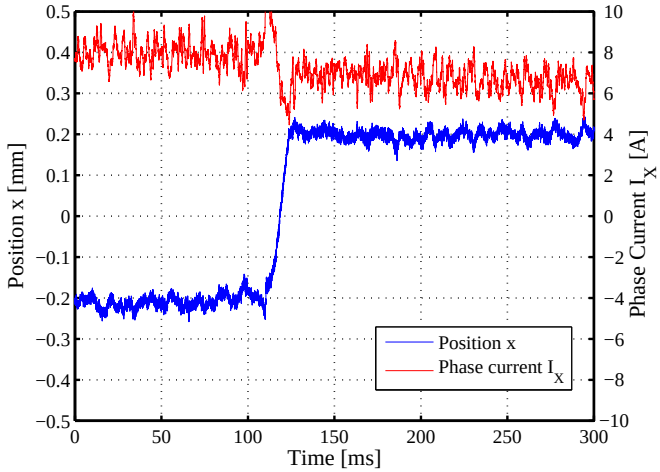

Figure 14. Sensorless movement from x=-0.2mm to x=-0.2mm and Phase current I_X, setup with $N_M = 24$ ferrite magnets at $U_{DC} = 120\,\mathrm{V}$

at centered rotor position is shown in Fig. 16. Compared to the single pulse strategy from the symmetric and the asymmetric sequence the three active INFORM results directly in a complete position information of all three coils after one INFORM pulse. Thus the information evaluation rate for one coil is three times higher compared to the symmetric and asymmetric INFORM sequences. Thus an increased sensing bandwidth at a low position noise is achieved. Here even with the low position sensing noise oscillations in the rotor position are identified.

Considering the overall control behavior of the sensorless three phase HMB system for different pre magnetization and INFORM sequences, a design compromise between bias current consumption and self sensing accuracy is identified in this

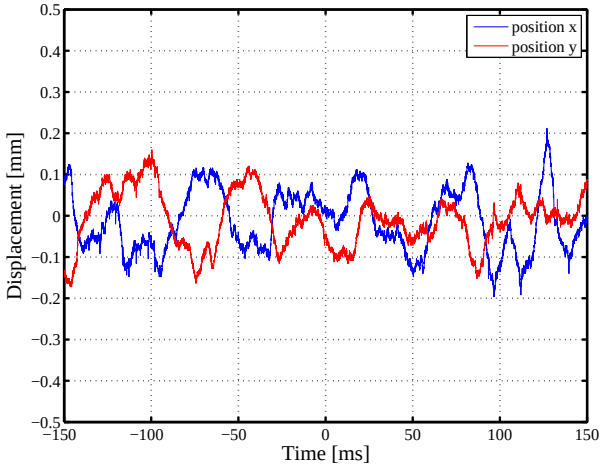

Figure 15. Sensorless operation with asymmetric INFORM pulses with 8 samples at centered rotor, setup with a combination of 12 ferrite and 12 NdFeB magnets at $U_{DC} = 120\,\mathrm{V}$

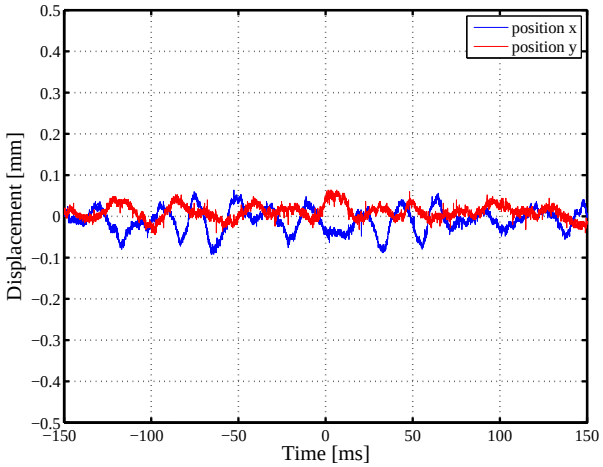

Figure 16. Sensorless operation with three active INFORM pulses with 16 samples at centered rotor, setup with a combination of 12 ferrite magnets and 12 NdFeB magnets at $U_{DC} = 120\,\mathrm{V}$

work. The reason is, that a higher bias flux is recommended to reduce the current consumption in operation, but this negatively affects the sensorless accuracy in an indirect way. Although the position detection noise does not change due to a higher bias flux, but bearing parameters K_x and K_i change. Thus, with the required increase of the controller gain increase the noise in the closed loop system is amplified. To overcome this trade off a further reduction of self sensing position noise is required. A first improvement can be the integration of the three active INFORM pulse sequence directly into the PWM voltage pattern of the current control as described in [9]. The self-sensing bandwidth gets increased and control behavior is expected to be improved. Because the operational modes of current control and position measurement do not work sequentially by interrupts and they are merged and distortions of the current control get reduced. Additionally, an eddy current reduction by utilization of enhanced lamination materials improves the position signal noise by increasing the "linear" range of the current slope measurement.

VI. Conclusions

In this paper new results and improvements regarding the sensorless position detection and sensorless position control of a three phase permanent magnet biased radial AMB are presented. Following concluding statements are identified:

- Utilizing oversampling strategies in the DSP increases the accuracy of the current slope measurement and consequently the sensorless rotor position noise is reduced and sensing accuracy is improved.
- Alternative INFORM pulse sequences allow an increase of position sensing frequency and result in a higher possible control bandwidth. At the three active sequence a rotor position is immediately available after one interruption. Additionally this sequence show the lowest position noise.
- A dependency of the sensorless rotor position detection method from the bias flux level was not identified in the open loop, but changed bearing parameters and increased control gain affect the overall behavior. A high sensibility of the position noise is given which result in oscillations at levitated operation.

Although this AMB prototype setup show limitations for self sensing especially at high bias flux for reaching low current consumption, two possible improvements are identified. First, reducing eddy currents for increased signal utilization and second, integrating the three active INFORM pulse sequence in a three active PWM control pattern. These topics will be investigated in future research work.

VII. Acknowledgment

This work is conducted within the project P21631-N22 of the Vienna University of Technology with the Austrian Science Fund (FWF). The authors thank the Austrian Science Fund for supporting this project.

References

[1] G. Schweitzer, *Magnetic Bearings, Theory, Design, and Application to Rotating Machinery*. Springer Berlin, 2009.

[2] E. Malsen, "Selfsensing for active magnetic bearings: overview and status," in *Proceedings of the Tenth International Symposium on Magnetic Bearings (ISMB10)*, 2006.

[3] M. Hofer, W. Staffler, and M. Schrödl, "Sensorless control of a three phase radial active magnetic bearing," in *Proceedings of the Twelfth International Symposium on Magnetic Bearings (ISMB12)*, 2010, pp. 680–685.

[4] M. Hofer, "Design and sensorless position control of a permanent magnet biased radial active magnetic bearing," Ph.D. dissertation, Vienna University of Technology, June 2013.

[5] D. Montie, "Performance limitations and self-sensing magnetic bearings," Ph.D. dissertation, University of Virginia, 2003.

[6] M. D. Noh and E. H. Maslen, "Self-sensing magnetic bearings (part ii) - effects on saturation," in *Proceedings of the Fifth International Symposium on Magnetic Bearings (ISMB5)*, Aug. 1996, pp. 113–118.

[7] H. Zhu, H. Chen, Z. Xie, and Y. Zhou, "Configuration and control for ac-dc three degrees of freedom hybrid magnetic bearings," in *Proceedings of the Tenth International Symposium on Magnetic Bearings (ISMB10)*, 2006.

[8] M. Hofer and M. Schrödl, "Statistic properties of a sensorless control method for a three phase permanent magnet biased radial active magnetic bearing," in *Proceedings of the 13th European Conference on Power Electronics and Applications (EPE 2009)*, 2009.

[9] T. Nenning, M. Hofer, M. Hutterer, and M. Schrödl, "Setup with two self-sensing magneitc bearings using differential 3-active inform," in *Proceedings of the Fourteenth International Symposium on Magnetic Bearings (ISMB14)*, 2014.